Contents lists available at ScienceDirect

Computers & Graphics

journal homepage: www.elsevier.com/locate/cag

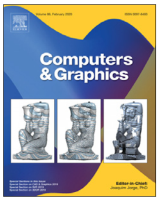

Technical Section

A weakly supervised framework for real-world point cloud classification[☆]

An Deng [a,b], Yunchao Wu [b], Peng Zhang [a], Zhuheng Lu [a], Weiqing Li [c], Zhiyong Su [a,*]

[a] *School of Automation, Nanjing University of Science and Technology, Nanjing, 210094, China*
[b] *Science and Technology on Information System Engineering Laboratory, Nanjing, 210007, China*
[c] *School of Computer Science and Engineering, Nanjing University of Science and Technology, Nanjing, 210094, China*

ARTICLE INFO

Article history:
Received 2 August 2021
Received in revised form 21 December 2021
Accepted 22 December 2021
Available online 30 December 2021

Keywords:
Weakly supervised learning
Real-world point cloud
Point cloud classification
Point cloud segmentation

ABSTRACT

Real-world point cloud objects pose great challenges in point cloud classification as objects acquired by scanning devices from real-world scans are often cluttered with background, and are partial due to occlusions as well as reconstruction errors. In the literature, few works tackle the problem of real-world point cloud classification while existing methods require fully point-level annotated training samples. However, large-scale dense point-level foreground–background labeling for real-world point clouds is a labor-intensive and time-consuming job. Leveraging two auxiliary modules, called semi-supervised point-level pseudo labels generation and noise-robust multi-task loss, the framework can integrate well with existing supervised point cloud classification network. A relational graph convolutional network on the local and non-local graph (PointRGCN) is first proposed to predict point-level foreground–background pseudo labels for each object with sparse ground-truth point-level foreground–background labels in training datasets. Then, a weakly supervised classification network, which combines with an auxiliary foreground–background segmentation branch, is employed to classify real-world point clouds. To cope with noise-containing point-level foreground–background labels generated above, a noise-robust multi-task loss is proposed to train the network accurately. Experimental results show that the performance of the proposed framework which is trained with only 1% point-level labels is comparable with many popular or state-of-the-art fully supervised methods. The source code will be available at http://zhiyongsu.github.io.

1. Introduction

Point cloud object classification, which is a classical and critical problem in computer graphics and computer vision fields, aims to identify the categories of different point cloud objects [1,2]. The rapid development of scanning devices has witnessed the wide application of point clouds in the fields of robotics, autonomous vehicles, augmented reality, urban planning, industrial manufacturing applications, etc [3–5]. Many works in the literature have made great progress in the synthetic 3D point cloud classification task [1,6,7]. Specially, the overall accuracy of the state-of-the-art methods on ModelNet40, the most popular synthetic point cloud dataset for classifying point cloud objects, has reached more than 94% in 2021 [8], and the trend of bringing the accuracy towards perfection is still ongoing.

However, recent studies show that the classification models trained on synthetic datasets often do not generalize well to real-world point cloud objects [9,10]. Synthetic datasets are usually generated with the assumption that objects are complete, clean, and especially free from any background noise. Unfortunately, real-world point cloud objects, which are obtained through LiDAR sensors or RGBD scanners, may suffer from background points (surroundings), noise, and holes. These objects exhibit some confusing information, which increases the difficulty of classifying real-world point cloud. Consequently, applying existing point cloud classification methods to real-world objects may not achieve results as good as synthetic cases. Therefore, how to handle the background effectively when they appear together with objects due to clutter in the real-world scenes is still a very challenging task [9].

Up to now, only a few pieces of works target the real-world point cloud classification problem. They employ transfer learning [10], learning transformation invariant representation [11,12], and multi-task learning [9]. Transfer learning-based method attempts to employ extra synthetic data to enrich standard feature representations [10]. Some works try to learn translation and rotation to adapt real-world point clouds that are not well aligned [11,12]. However, none of these works have considered the background points which is the most challenging problem

[☆] This article was recommended for publication by B. Preim.
[*] Corresponding author.
E-mail address: su@njust.edu.cn (Z. Su).

https://doi.org/10.1016/j.cag.2021.12.008

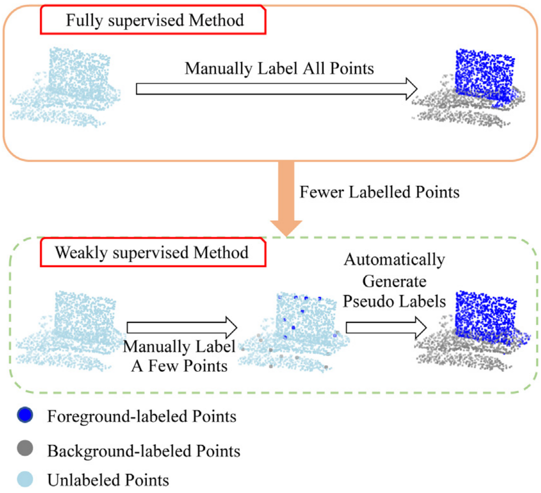
Fully supervised Method
Manually Label All Points
Fewer Labelled Points
Weakly supervised Method
Automatically Generate Pseudo Labels
Manually Label A Few Points
● Foreground-labeled Points
● Background-labeled Points
● Unlabeled Points

Fig. 1. Illustration of the real-world point cloud contaminated by background points, and the weak supervision concept in this work. Our weakly supervised approach assists real-world point cloud classification with fewer foreground–background labeled points.

of real-world point cloud classification. Multi-task learning-based method benefits the real-world point cloud classification network through distinguishing foreground and background points with an auxiliary segmentation task [9]. However, it requires accurate dense point-level foreground–background labels (annotations). Despite recent developments of modern annotation toolkits [13–15], exhaustive labeling is still a quite labor intensive and time-consuming job for ever-growing new datasets.

In this paper, we propose a novel weakly supervised classification framework, called WSC-Net, for classifying real-world point clouds. This concept contains incomplete supervision and inaccurate supervision [16]. Specifically, the framework is designed to take advantage of and integrate well with existing supervised point cloud classification networks through introducing two auxiliary modules : semi-supervised point-level pseudo labels generation and noise-robust multi-task loss. The former aims to generate point-level foreground–background pseudo labels for each object in training datasets with sparse ground-truth point-level foreground–background labels, as illustrated in Fig. 1. Undoubtedly, noisy labels will be inevitably introduced during this stage. The latter strives to fade away their negative effects to train the classification network efficiently and accurately. Compared with existing real-world point cloud classification methods, our method can yield competitive performance without the need of tedious and time-consuming labeling processes for preparing training data.

In summary, the main contributions of this paper are as follows:

- A novel weakly supervised framework for real-world point cloud object classification is proposed. The framework can make full use of existing supervised networks by incorporating semi-supervised pseudo labels generation and noise-robust multi-task loss.
- A local and non-local graph-based relational graph convolutional network (PointRGCN) is proposed to generate point-level foreground–background pseudo labels for each object in training datasets in a semi-supervised manner. By applying the PointRGCN, each point can aggregate more discriminative features from multi-type of neighbors, resulting in more accurate point-level pseudo labels.
- A noise-robust multi-task loss that combines classification and segmentation losses is proposed to train the classification network accurately with noise-containing point-level foreground–background labels.
- We demonstrate that our WSC-Net framework produces comparable results with the state-of-the-art fully-supervised approaches with only 1% point-level labels.

The remaining of this paper is organized as follows: In Section 2, we compare the differences between synthetic and real-world point cloud classification works, and then briefly introduce the work related to weakly supervised learning on point cloud and noisy label learning. Section 3 gives an overview of the proposed weakly supervised real-world point cloud classification framework. Problem Formulation is discussed in Section 4. We introduce the proposed PointRGCN and noise-robust multi-task loss in detail in Sections 5 and 6, respectively. After that, we present the experimental results of the proposed weakly supervised real-world point cloud classification method in Section 7. Finally, conclusions and suggestions for future research are provided in Section 8.

2. Related work

2.1. Synthetic point cloud classification

Early attempts at point cloud classification generally focused on the ideal synthetic point cloud data. Overall, synthetic point cloud classification methods can be subdivided into projection-based, voxel-based, and point-based methods. Projection-based methods need to project the original point cloud onto 2D images and use 2D CNNs to process them [17–19]. These methods are also called multi-view based methods. Since multi-view based methods need to render batches of 2D images, it will lose the intrinsic geometric features of the point cloud. Recently, Goyal et al. [20] proved that even a projection-based method can perform well with careful data augmentation strategies and appropriate loss functions. Voxel-based methods usually voxelize point clouds into 3D grids, then feed them to CNNs [21,22]. However, 3D CNNs are very computationally expensive, hence the resolution of point clouds is highly limited. Alternatively, point-based methods can directly handle 3D point clouds. According to the different ways of point feature learning, these methods can be divided into Multi-layer Perceptron-based (MLP-based), graph-based, and point convolution-based methods. MLP-based methods learn 3D point cloud features through multi-layer perceptrons (mlps), capture local geometric features by aggregating neighboring information, and use symmetric functions to aggregate features of all points to form a global shape descriptor [1,6, 23,24]. Graph-based methods [25–32] represent the point cloud as a graph by considering the points as nodes, and constructing links between points as edges. The graph neural network defined in the spectral domain or the spatial domain is then employed to process point cloud objects. Recently, point convolution operators [7,33–40] were proposed to apply convolution operations on point clouds directly.

Nevertheless, the aforementioned point cloud classification methods only focus on synthetic point cloud data, and do not consider real-world point cloud data contaminated by background points. Due to the characteristics of real-world point clouds, existing works that tend to be perfect on ideal synthetic point cloud data cannot work well on real-world data.

2.2. Real-world point cloud classification

Currently, there are only a handful of works that consider the classification of real-world point cloud objects. Uy et al. [9] proposed a background-aware (BGA) model to handle the occurrence of background points in point clouds obtained from real scans, but this method requires dense point-level foreground–background labels. A method that joints supervised and self-supervised learning was proposed by Alliegro et al. [10]. It enriches features by jointly learning a supervised main classification model and a self-supervised 3D puzzle which is to reassemble the split point cloud. Since it does not directly address the impact of background points on real-world point cloud classification tasks, the performance is still unsatisfying. Zhao et al. [12] proposed to combine local geometry with global topology to achieve rotation-invariant representations for the real-world point cloud. Fuchs et al. [11] presented an attention-based neural architecture which is robust against rotations and translations. It updates features using SE(3)-Transformer, an equivariant attention mechanism. These works have shown great potential in improving the robustness to geometric transformations, but none of them target at point clouds contaminated by the background.

In short, existing real-world point cloud classification methods either require complete foreground–background annotation point clouds as training data, or ignore the interference caused by background points to point cloud classification. Our method attempts to combine weakly supervised learning with real-world point cloud classification tasks. We try to handle real point clouds contaminated by background points through taking sparse point-level annotations as supervision.

2.3. Unsupervised and weakly supervised learning on point cloud

Unsupervised methods do not require labeled data, but most of them focus on low-level visual tasks, such as point clustering, and distinctive region detection. Li et al. [41] proposed to learn and detect distinctive regions on 3D shapes in an unsupervised manner. Self-supervised methods, as a popular branch of unsupervised learning, mainly focus on pretext tasks, which are proposed to learn feature representation in an unsupervised manner. However, the point-wise feature learned by pretext tasks cannot be directly used for downstream point cloud classification and segmentation tasks. MortonNet [42] learned point-wise features by leveraging space-filling curves in a self-supervised manner. Sauder et al. [43] proposed a self-supervised learning task to learn point cloud representations by training a model that reassembles randomly split point clouds. Recently, several works have tried to utilize less supervision to achieve point cloud semantic segmentation. A weakly supervised point cloud segmentation method proposed by Xu et al. [44] introduces additional losses to regularize the model. However, it adds a smooth branch to the original segmentation network, which will reduce the efficiency of the inference stage. Wei et al. [45] proposed a weakly supervised point cloud segmentation method that only uses scene-level weak labels and sub-cloud weak labels. Yet this work only focuses on large scenes with many different types of objects, it cannot be extended to part segmentation tasks.

Overall, it is hard to directly apply these methods to classify real-world point cloud objects. These methods are also difficult to be directly and efficiently integrated into existing point cloud classification approaches.

2.4. Robust learning with noisy labels

In practical applications, it is unrealistic to always obtain completely clean labeled data. To this end, many approaches have been proposed to learn with noisy labels, such as correcting noise labels, using adaptive training strategies, modifying loss functions, and using noise-robust loss function. There are several attempts which use conditional random field [46], neural network [47], knowledge graph [48], and other methods to correct wrong labels. However, those approaches require additional clean label data. Another scenario is to design adaptive training strategies that are more robust to noisy labels [49–51]. Some approaches enhance the robustness of the model to noisy labels by modifying the loss function. Han et al. [52] estimated a noise transformation matrix that defines the probability of mislabeled classes with other classes [53]. It has been proven that the Mean Absolute Error (MAE) is robust to noisy labels, but the commonly used Cross Entropy (CE) loss is not [54]. However, the robustness of MAE will increase the difficulty of training. The Generalized Cross Entropy (GCE) loss proposed by Zhang et al. [55] can be seen as a generalization of MAE and CE. Wang et al. [56] proposed the Symmetric Cross Entropy (SCE) which combines a Reverse Cross Entropy (RCE) with the CE loss. It strikes a balance between sufficient learning and robustness against noisy labels.

3. Overview of the framework

The proposed WSC-Net framework for real-world point cloud classification consists of two stages, as illustrated in Fig. 2. In the first stage, to produce extra supervision from limited labeled points, we propose a novel semi-supervised PointRGCN to generate pseudo foreground–background labels for each incompletely labeled real-world point cloud object. A k-NN voting-based smoothness constraint module is introduced to refine pseudo labels, since the generated pseudo labels contain some misclassifications. In the second stage, a weakly supervised real-world point cloud classification network is employed to classify real-world point cloud. To accurately train the final classification model, a novel multi-task noise-robust loss constrained on shape-level labels, point-level sparse labels, and noisy pseudo labels is introduced. The filtered points are only used for feature extraction, and the loss of these points is ignored.

4. Problem formulation

We consider a point cloud dataset with B samples and K classes as $\{\mathbf{X}_b\}_{b=1,2,3,\dots,B}$. Each sample $X_b \in \mathbb{R}^{N\times F}$ consists of N 3D points with its xyz coordinates and other additional attributes, e.g., surface normal and RGB values, where each surface normal represents a vector perpendicular to the tangential plane fitted by each point and its neighbors, and RGB values reveal the color information of each point. Each sample X_b is accompanied with a shape-level class label $V_b \in \{1,\dots K\}$ which is easy to obtain, and it is further accompanied with ground-truth point-level foreground–background label $y_b \in \{0,1\}^S$, where 0 and 1 represent the background and foreground point respectively, S is the number of points with ground-truth point-level labels, $S \ll N$. We denote the one-hot encoded shape-level label and point-level labels as $\hat{V}_b$ and $\hat{y}_b$, respectively. We assume that only S points of each training sample are labeled. Therefore, we define a binary mask $M \in \{0,1\}^{B\times N}$. For each point x_i in sample X_b, $m_{bi} = 0$ means that x_i is unlabeled, otherwise it has a ground-truth label. A semi-supervised relational graph convolutional neural network $h(\mathbf{X};\Theta_1)$, parameterized by Θ_1, is designed to generate pseudo labels for each sample X_b. A point cloud encoder network $f(\mathbf{X};\Theta_2)$, e.g., DGCNN [6], PointNet++ [23], parameterized by Θ_2, is employed to obtain the embedded point cloud features $Z_e \in \mathbb{R}^{N\times H}$.

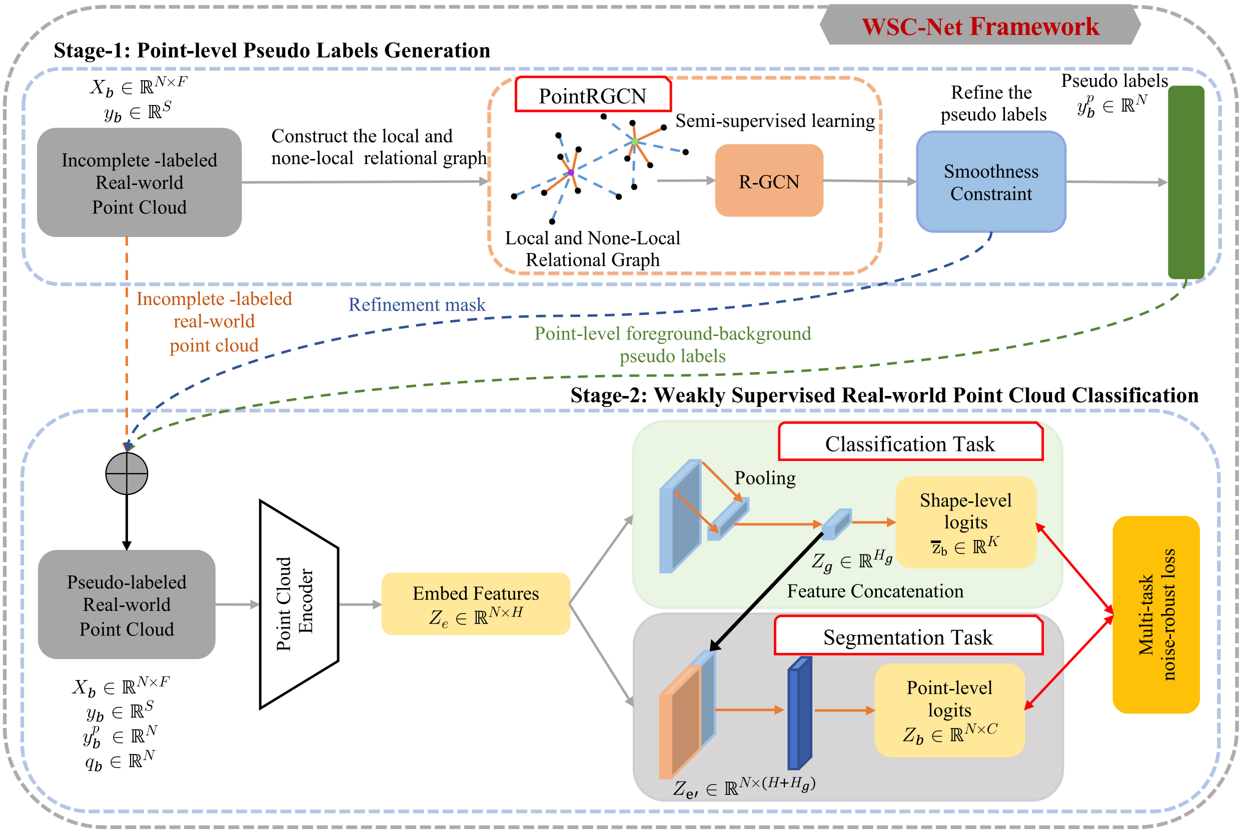
WSC-Net Framework
Stage-1: Point-level Pseudo Labels Generation
$X_b \in \mathbb{R}^{N\times F}$
$y_b \in \mathbb{R}^{S}$
Incomplete -labeled Real-world Point Cloud
Construct the local and none-local relational graph
PointRGCN
Semi-supervised learning
R-GCN
Local and None-Local Relational Graph
Refine the pseudo labels
Smoothness Constraint
Pseudo labels $y_b^p \in \mathbb{R}^N$
Incomplete -labeled real-world point cloud
Refinement mask
Point-level foreground-background pseudo labels
Stage-2: Weakly Supervised Real-world Point Cloud Classification
Pseudo-labeled Real-world Point Cloud
$X_b \in \mathbb{R}^{N\times F}$
$y_b \in \mathbb{R}^{S}$
$y_b^p \in \mathbb{R}^N$
$q_b \in \mathbb{R}^N$
Point Cloud Encoder
Embed Features $Z_e \in \mathbb{R}^{N\times H}$
Classification Task
Pooling
Shape-level logits $\overline{z}_b \in \mathbb{R}^K$
$Z_g \in \mathbb{R}^{H_g}$
Feature Concatenation
Segmentation Task
Point-level logits $Z_b \in \mathbb{R}^{N\times C}$
$Z_{e'} \in \mathbb{R}^{N\times(H+H_g)}$
Multi-task noise-robust loss

Fig. 2. The proposed weakly supervised real-world point cloud classification framework.

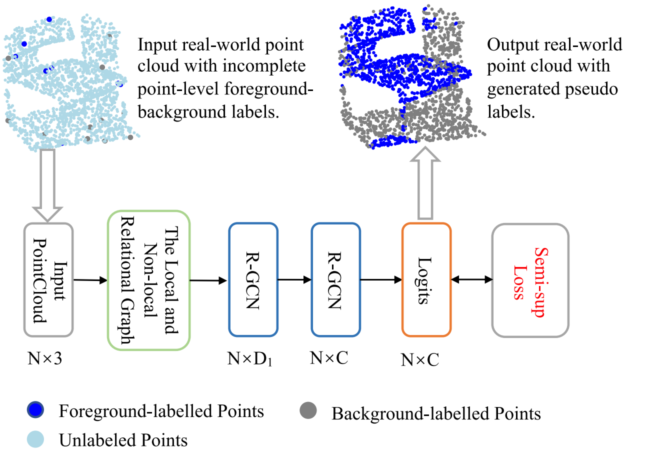
Input real-world point cloud with incomplete point-level foreground-background labels.
Output real-world point cloud with generated pseudo labels.
Input PointCloud
The Local and Non-local Relational Graph
R-GCN
R-GCN
Logits
Semi-sup Loss
N×3
N×D₁
N×C
N×C
Foreground-labelled Points
Background-labelled Points
Unlabeled Points

Fig. 3. Illustration of the proposed PointRGCN for point-level pseudo labels generation with a per-point loss function.

5. Point-level pseudo labels generation

In this section, to produce extra supervision for the classification model training, we firstly propose a PointRGCN to generate point-level foreground–background pseudo labels for the incompletely labeled real-world point cloud, as shown in Fig. 3. The proposed PointRGCN consists of two parts: the local and non-local relational graph construction, and a semi-supervised relational graph convolutional network (R-GCN). A smoothness constraint module is introduced to filter suspicious pseudo labeled points.

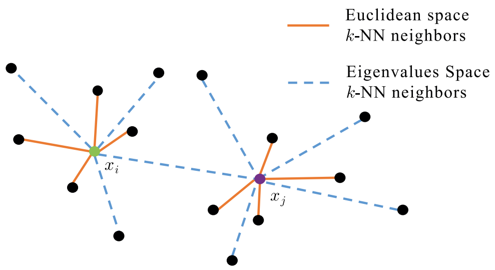
Euclidean space k-NN neighbors
Eigenvalues Space k-NN neighbors
x_i
x_j

Fig. 4. Illustration of the local and non-local relational graph. Different colored lines indicate different types of neighborhoods.

5.1. The local and non-local relational graph construction

To extract more discriminative point cloud features, we construct a local and non-local relational graph to aggregate local and non-local information of each point, as shown in Fig. 4. Specifically, the local relational graph is defined in the Euclidean space, while the non-local relational graph is defined in the Eigenvalues space. Currently, the common methods used to construct the graph for a point cloud, such as searching the k-nearest neighbors in the Euclidean space [1,6,57] (k-NN graph) or searching neighbors in a fixed metric radius sphere [23,27] (radius graph), can only aggregate point features in a local way. As a result, the extracted features of points on the local graph tend to be smoothed. Therefore, to avoid over-smoothing features and generate pseudo labels with higher quality, for each point, we choose to not only aggregate its k-nearest neighbors in the Euclidean space, but also aggregate the points which have similar local geometric features but located distantly in the Euclidean space [2].

Algorithm 1: PointRGCN, Point-level Pseudo Labels Generation

```
Input: Point cloud $\{X_b \in \mathbb{R}^{N\times F}\}$, labels $\{y_b \in \mathbb{Z}^S\}$
Output: Pseudo labels predictions $\{y_b^p \in \mathbb{Z}^N\}$
/* The Local and Non-local Relational Graph
   Construction:                                              */
Search $k_1$-nearest neighbors in the Euclidean space to get local
  neighbors;
Search $k_2$-nearest neighbors in the Eigenvalue space to get
  non-local neighbors;
Construct the local and non-local relational graph according to
  Eqs. (2) and (3);
/* Semi-Supervised R-GCN                                      */
for $Epoch \leftarrow 1$ to $Epochs$ do
  | Train the R-GCN for one epoch: $\Theta_1 = \Theta_1 - \alpha\nabla\mathcal{L}_{semi}|_{\{X_b\},\{y_b\}}$;
end
/* Obtain Predictions:                                        */
Forward pass $Z_h = h(X_b; \Theta_1)$;
Obtain pseudo labels predictions $y_b^p$ via $\mathrm{argmax}_i\, z_{hi}$ .
```

Algorithm 2: Smoothness Constraint

```
Input: Point cloud $\{X_b \in \mathbb{R}^{N\times F}\}$, pseudo labels $\{y_b^p \in \mathbb{Z}^N\}$
Output: Refinement mask $\{Q_b \in \mathbb{R}^N\}$;
for $x_i : X_b$ do
    /* Obtain Majority Predictions                                */
    Search $k$-nearest-neighbors in the Euclidean space for $x_i$;
    Find the most frequent label in the collection of $x_i$'s $k$-NN
      neighbors' pseudo labels $\mathbf{y}_{\mathcal{N}_i}$, written as $y_{bi'}$ (majority
      prediction).
    /* Construct Refinement Mask Based on Majority
       Prediction                                                 */
    if $y_{bi'} = y_{bi}^p$ then
      | $q_{bi} = True$;
    else
      | $q_{bi} = False$;
    end
end
```

Firstly, we use the k-NN algorithm to get the k_1-nearest neighbors of each point x_i in the Euclidean space, written as $\mathcal{N}_i^{local}$. Then, following [2], we get the k_2 non-local neighbors of each point x_i in the Eigenvalues space, written as $\mathcal{N}_i^{non-local}$. The k_1-nearest neighbors of point x_i is $\{x_{i1}, x_{i2}, \dots, x_{ik_1}, x_{ik_1} \in \mathcal{N}_i^{local}\}$. Let $U = \{x_{i1} - x_i, x_{i2} - x_i, \dots, x_{ik_1} - x_i\}$, then define $C = U^T \times U$. We have the decomposition $C = R\Lambda R^T$, where R is the rotation matrix, and Λ is a diagonal and positive definite matrix, known as eigenvectors and eigenvalues matrixes respectively [2]. Eigenvalues of each point x_i can be represented as $\lambda_i \in \mathbb{R}^3$, and ordered as $\lambda_i^1 \geq \lambda_i^2 \geq \lambda_i^3$. We use L^2 distance to calculate the distance in the Eigenvalues space between different points. Then, we choose the k_2 nearest neighbors for each point x_i according to

$$Distance(x_i, x_j) = \|\lambda_i - \lambda_j\|. \tag{1}$$

Finally, by properly arranging these two types of neighbors, each point can capture richer local and non-local information. We unite the local neighbors $\mathcal{N}_i^{local}(1 \leq i \leq N)$ and non-local neighbors $\mathcal{N}_i^{non-local}(1 \leq i \leq N)$ to form the local and non-local relational graph, represented as $\mathcal{N}_i^r(1 \leq i \leq N, r \in \{local, non-local\})$.

We define the adjacency matrix of the local and non-local relational graph as:

$$A = \begin{bmatrix} c_{00} & \dots & c_{0N} \\ & \vdots & \\ c_{N0} & \dots & c_{NN} \end{bmatrix}, \tag{2}$$

where c_{ij} indicates whether there is a relation between x_i and x_j. $c_{ij} = 1$ if x_j is the neighbor of x_i, otherwise $c_{ij} = 0$. According to the different types of neighborhood relations between x_i and x_j, we can build the edge type matrix E as:

$$E = \begin{bmatrix} e_{00} & \dots & e_{0N} \\ & \vdots & \\ e_{N0} & \dots & e_{NN} \end{bmatrix}, \tag{3}$$

where e_{ij} denotes the relational type of x_i and x_j. We have $e_{ij} \in \mathcal{E}$, and the types of all relations in the local and non-local relational graph form the relation type set $\mathcal{E} = \{local, non-local\}$.

5.2. Semi-supervised relational graph convolutional networks

In order to extract richer information from multiple relation types of neighbors for each point, we introduce a relational graph convolutional network (R-GCN) [58] to generate pseudo foreground–background labels in a semi-supervised manner. R-GCN uses multiple groups of weights to learn feature transformations between different relation types. The proposed PointRGCN consists of two R-GCN layers (defined in Eq. (4)), and the output of the previous layer is the input to the next layer [58]. In the first layer, it takes the local and non-local relational graph as input, then extracts high-level point features $Z_h^1 \in \mathbb{R}^{N\times D}$. In the second layer, the embedded features Z_h^1, after passing a ReLU activation, is mapped to prediction scores $Z_h \in \mathbb{R}^{N\times 2}$. The forward propagation formula of the R-GCN layer can be written as:

$$Z_{hi}^{(l+1)} = \sigma\left(\sum_{r\in\mathcal{E}}\sum_{j\in\mathcal{N}_i^r}\frac{1}{c_{i,r}}W_r^{(l)}Z_{hj}^{(l)} + W_0^{(l)}Z_{hi}^{(l)}\right), \tag{4}$$

where $Z_{hi}^{(l)}$ is the hidden state of point x_i in the lth layer, $j \in \mathcal{N}_i^r$ denotes the set of neighbors of point x_i under the relation type r, $c_{i,r}$ is a problem-specific normalization constant which is set to $|\mathcal{N}_i^r|$ in this paper, and W is a learnable weight matrix.

The optimization objective Eq. (5) is penalized only on ground-truth labeled points, while ignoring unlabeled points. We minimize the per-point softmax cross-entropy loss only on labeled points:

$$\mathcal{L}_{semi} = -\sum_i m_{bi}\sum_k \hat{y}_{bik}\log\frac{\exp(z_{hik})}{\sum_k \exp(z_{hik})}, \tag{5}$$

where m_{bi} indicates whether point x_i is labeled or not, which means the semi-supervised R-GCN is constrained with only a few labeled points $\hat{y}_b \in \{0, 1\}^{\{S\times 2\}}$, z_h is the logits on foreground and background. Through multiple epochs of training, each point can obtain more discriminative fine-grained features from the local and non-local relational graph, and the unlabeled points can get the predicted pseudo labels.

The proposed pseudo labels generation algorithm is shown in Algo. 1.

5.3. Smoothness constraint

A k-NN voting-based smoothness constraint module is introduced to filter out suspicious pseudo labels, and further refine the generated pseudo labels. Although the PointRGCN can generate high-quality predicted labels for the majority of unlabeled points, the prediction is not perfect. To alleviate the negative impact of wrongly labeled points, we introduce a k-NN voting-based method to filter out suspicious points. We count the number of different types of labels in the one-hot k-NN neighborhood of

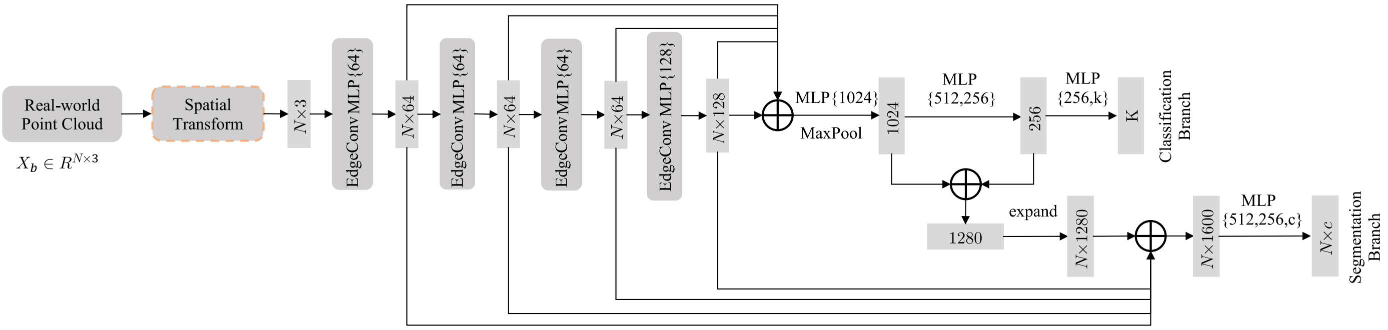

Fig. 5. Weakly supervised real-world point cloud classification network.

each point x_i. If the pseudo label of x_i is inconsistent with the mode of its k-NN neighbors' pseudo labels, it is considered as an invalid labeled point. A binary refinement mask $\mathbf{q} \in \{0, 1\}^{B\times N}$ can be obtained through the k-NN voting mechanism to indicate whether a point is valid or not. For each point x_i, it is invalid if $q_{bi} = 0$, otherwise it is valid. The k-NN voting-based smoothness constraint algorithm is summarized in Algo. 2.

6. Weakly supervised real-world point cloud classification network

In this section, we firstly present a weakly supervised real-world point cloud classification network architecture which is employed to classify real-world point cloud, with the assistance of an auxiliary weakly supervised segmentation task. Then, we present the noise-robust multi-task loss to train the classification model accurately on noisy pseudo labels.

6.1. Network architecture

The weakly supervised real-world point cloud classification network architecture, as depicted in Fig. 5, consists of a classification branch and a weakly supervised foreground–background segmentation branch, inspired by the fully supervised background-aware (BAG) classification network [9]. The classification branch is trained on shape-level labels. The segmentation branch is trained on both few point-level ground-truth labels and generated pseudo labels. Unlike BAG [9] which assists classification through a fully supervised segmentation branch, our method employs a weakly supervised segmentation branch.

We choose DGCNN [6] as the backbone network to extract point cloud features, due to its impressive performance in both point cloud classification and segmentation tasks. In the classification branch, point cloud features Z_e are aggregated into a 1-D global feature, i.e. $Z_g = \max_i Z_{ei}$, to produce object classification scores $\bar{z}_b \in \mathbb{R}^K$ through several fully connected layers. In the segmentation branch, the expanded global feature $Z_{g'} \in \mathbb{R}^{N\times H_g}$ and point-level features Z_e are concatenated as $Z_{e'}$ to obtain point-level segmentation scores $Z_b \in \mathbb{R}^{N\times C}$.

The classification branch is constrained on shape-level labels, and the segmentation branch is constrained on a small number of ground-truth labels and generated pseudo labels. We train both classification and foreground–background segmentation branches jointly with noisy label learning.

6.2. Noise-robust multi-task loss

To accurately train the weakly supervised real-world point cloud classification network, we propose a noise-robust multi-task loss that combines both classification loss and noise-robust segmentation loss. The combined classification-segmentation loss is:

$$\mathcal{L}_{total} = \mathcal{L}_{cls} + \lambda \mathcal{L}_{seg}, \tag{6}$$

where λ is used to balance the classification task and segmentation task.

For the classification branch, we firstly use a channel-wise symmetric aggregation operation [6] on the embedded feature, i.e. $z_b = max_i(z_{bi})$. Then, we use several fully connected layers to obtain $\tilde{z}_b$, the logits on each object category. We apply a softmax Cross Entropy (CE) loss for the classification branch. Consequently, the classification loss can be defined as:

$$\mathcal{L}_{cls} = -\sum_k \hat{V}_{bk} \log \frac{\exp(\bar{z}_{bk})}{\sum_k \exp(\bar{z}_{bk})}, \tag{7}$$

where $\hat{V}_b$ is the one-hot encoded shape-level label.

For the segmentation branch, since the refined pseudo labels still contain a small amount of misclassification, we propose a segmentation loss $\mathcal{L}_{seg}$ which is tolerant to noisy pseudo labels. The proposed loss $\mathcal{L}_{seg}$ contains two terms: the segmentation loss on the weak labels, and the segmentation loss on the pseudo labels. Hence, the segmentation loss $\mathcal{L}_{seg}$ can be written as:

$$\mathcal{L}_{seg} = \mathcal{L}_{weak} + \mathcal{L}_{pseudo}. \tag{8}$$

$\mathcal{L}_{weak}$ that penalizes weak labels can be specifically written as:

$$\mathcal{L}_{weak} = -\sum_i m_{bi} \sum_k \hat{y}_{bik} \log \frac{\exp(z_{bik})}{\sum_k \exp(z_{bik})}, \tag{9}$$

where z_b is the point-level logits on each segmentation category, m_{bi} indicates whether point x_i has a ground-truth label, and $\hat{y}_b$ is the one-hot encoded point-level labels.

Due to the corruption of pseudo labels, it is difficult to train an accurate real-world point cloud segmentation branch only with pseudo labels. Meanwhile, an inaccurate segmentation branch will not help the real-world point cloud classification, and will even degrade the classification performance. It has been demonstrated that the CE loss commonly used in the point cloud segmentation task is not robust against noisy labels [53,54]. Therefore, we introduce a noise-robust Symmetric Cross Entropy (SCE) [56] loss function to accurately train the segmentation branch with pseudo labels. The SCE loss consists of a Reverse Cross Entropy (RCE) term and a CE term. The RCE term is noise tolerant under symmetric or uniform label noise if the noise rate $\eta < 1 - \frac{1}{K}$, while the CE term is employed to achieve good convergence. The SCE is formally written as:

$$\begin{aligned}\mathcal{L}_{pseudo} &= \mathcal{L}_{ce} + \mathcal{L}_{rec}\\ &= -\sum_i (\neg m_{bi}) \wedge (q_{bi})\end{aligned}$$

Algorithm 3: Weakly Supervised Real-world Point Cloud Classification via Pseudo Labels Generation and Noise-robust Multi-task Loss

```
Input: Training dataset:
Point cloud in the training set$\{X_b \in \mathbb{R}^{N \times F}\}$ ;
A few point-level labels$\{y_b \in \mathbb{Z}^S\}$
Testing dataset:
Point cloud in the testing set$\{\tilde{X}_b \in \mathbb{R}^{N \times F}\}$
Output: Category predictions$\{\tilde{V}_b \in \mathbb{Z}\}$
/* Training Stage:                                  */
Generate point-level pseudo labels $\{y_b^p \in \mathbb{Z}^N\}$ according to Algo. 1;
Calculate refinement mask $\{Q \in \mathbb{R}^N\}$ according to Algo. 2;
for Epoch ← 1 to 150 do
    Train one epoch: $\Theta_2 = \Theta_2 - \alpha \nabla \mathcal{L}_{total}|_{\{X_b\},\{y_b\},\{\tilde{y}_b\},\{Q\}}$;
end
/* Inference Stage:                                 */
Forward pass $Z_p = h(\tilde{X}_b)$;
Obtain the final prediction via $\tilde{V}_b = \arg\max_k z_{pk}$.
```

$$\{\alpha_p \sum_k \hat{y}_{bik}^p \log \frac{\exp(z_{bik})}{\sum_k \exp(z_{bik})} + \beta_p \sum_k z_{bik} \log \frac{\exp(\hat{y}_{bik}^p)}{\sum_k \exp(\hat{y}_{bik}^p)}\} \tag{10}$$

where ¬ means logical negation, ∧ means logical and. q_{bi} means whether point x_i is valid, that is to say, $\mathcal{L}_{pseudo}$ only penalizes the valid pseudo labeled points. $\hat{y}_b^p$ is the one-hot encoded pseudo labels. α_p and β_p are hyperparameters, with α_p on the overfitting issue of CE while β_p for flexible exploration on the robustness of RCE [56].

The proper weights between $\mathcal{L}_{weakly}$ and $\mathcal{L}_{pseudo}$ are very critical for the final performance. Considering the number of weak labels is much less than that of pseudo labels, if we use the Eq. (8) directly, the segmentation branch will tend to fit noisy pseudo labels instead of the ground truth weak labels [59]. For the above reasons, the regularization is applied to re-weights the losses calculated on different labels to correct the impact of pseudo labels. The weighted segmentation loss function is:

$$\mathcal{L}_{seg} = \alpha \mathcal{L}_{weakly} + \beta \mathcal{L}_{pseudo}, \tag{11}$$

where α and β are parameters to balance the two terms. Then, the final segmentation loss $\mathcal{L}_{seg}$ is the weighted sum of the two terms. Since how to balance these two loss functions plays an important role on the final performance of the model [59], we assume $\beta \ll \alpha$ in this paper.

Finally, the classification loss and the noise-robust segmentation loss are combined as the noise-robust multi-task loss:

$$\mathcal{L}_{total} = \mathcal{L}_{cls} + \lambda(\alpha \mathcal{L}_{weakly} + \beta \mathcal{L}_{pseudo}). \tag{12}$$

7. Experiment

In this section, we firstly evaluate our WSC-Net on the ScanobjectNN [9] dataset. Then, we conduct detailed experiments to evaluate the importance of different modules and the compatibility with alternative backbone. We also visualize experimental results to analyze the effect of weakly supervised segmentation branch on the real-world point cloud classification network.

7.1. Implementation details

In the point-level pseudo labels generation stage, we train the R-GCN for 64 epochs, and the output of the final epoch is the predictions of pseudo foreground–background labels. To prevent over-fitting, the early stop strategy is adopted. That is to say, when the accuracy on the labeled points reaches 99% over 3 times, the training is stopped. Adam optimizer is used for efficient training. The initial learning rate is 0.0135, and we reduce the learning rate until 0.0001 using cosine annealing.

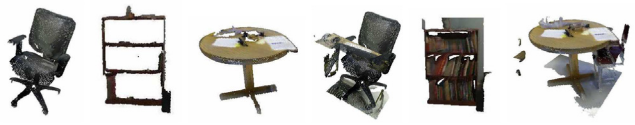

(a) Objects only. (b) Objects with background.

Fig. 6. Example objects from ScanobjectNN [9].

In the weakly supervised real-world point cloud classification stage, the training objective is the noise-robust multi-task loss function (Eq. (12)). We use an Adam optimizer as before, and the initial learning rate is 0.001. The exponential decay is applied to the learning rate. The batchsize is 32. We train the network for 150 epochs.

The number k_1 and k_2 of nearest neighbors in the local and non-local relational graph is set to 20, respectively. In the pseudo label refining step, we set the number k of nearest neighbors to 50 for the k-NN voting. The number k of nearest neighbors in DGCNN is 20.

Our weakly supervised real-world point cloud classification approach is summarized in Algo. 3.

7.2. Dataset

ScanobjectNN is the first and only real-world point cloud object dataset based on scanned indoor scene data with foreground–background annotations in the literature [9]. It consists of two types of data, namely the object point cloud with background, and the object point cloud only, as shown in Fig. 6. It is created from the state-of-the-art scene mesh datasets SceneNN [12] and ScanNet [60] in the way of automatically instance segmenting and manually filtering. And, it contains 15 common daily objects categories, such as tables, chairs, bookshelves, sinks, toilets, and displays.

Among the several variants of ScanObjectNN, we choose the most challenging one, the ScanObjectNN-PB_T50_RS, to evaluate our method. Each sample in this dataset randomly shifts the bounding box up to 50% of its size from the box centroid along each world axis. Meanwhile, rotation and scaling are applied to them [9]. ScanObjectNN-PB_T50_RS contains 13698 real-world point cloud objects from 15 categories. 11,416 objects are used for training and 2,282 objects are used for testing. Each point cloud object has 2048 points, and their coordinates are not normalized. Each point in the point cloud has a point-level label to indicate the foreground or background. We assume that only S points are labeled within each real-world point cloud sample. Specifically, in the following experiments, to avoid class imbalance, we uniformly sample 1% points from foreground and background parts respectively as supervision for each training object.

7.3. Evaluation metrics

For pseudo labels generation experiments, we calculate the segmentation accuracy for each sample and report the average segmentation accuracy over all instances (InsAvg) and all categories (CatAvg). The average refined segmentation accuracy over all instances is also reported as 'Re-InsAvg'. At the same

Table 1
The class-specific results of pseudo labels generated by PointRGCN with different levels of supervision.

Index	Model	Re-InsAvg	InsAvg	CatAvg	Bag	Bin	Box	Cabinet	Chair	Desk	Display	Door	Shelf	Table	Bed	Pillow	Sink	Sofa	Toilet
Acc	GCN_1%	82.78	82.18	82.28	84.61	**82.66**	80.82	81.68	84.14	75.39	85.28	84.42	**77.41**	83.25	81.36	81.94	**82.13**	**82.35**	**86.79**
	PointRGCN_1%	**84.86**	**82.49**	**82.57**	**85.08**	82.32	**81.24**	**82.94**	**84.35**	**75.91**	**85.40**	**85.61**	76.66	**84.07**	**81.60**	**82.51**	81.98	82.31	86.53
	GCN_10%	87.70	85.69	85.81	88.25	86.43	84.88	85.30	87.63	79.35	88.49	87.31	80.80	86.48	84.91	85.71	85.43	86.19	90.05
	PointRGCN_10%	**94.44**	**92.20**	**92.42**	**94.12**	**92.76**	**92.75**	**92.63**	**93.59**	**88.20**	**94.18**	**93.84**	**86.38**	**92.37**	**92.09**	**93.38**	**92.82**	**92.35**	**94.81**
mIoU	GCN_1%	–	61.81	62.43	66.97	64.11	61.51	61.33	65.24	52.58	65.80	61.16	52.56	59.61	62.64	64.91	63.54	63.60	70.91
	PointRGCN_1%	–	**64.46**	**64.93**	**69.22**	**65.07**	**63.96**	**65.35**	**67.29**	**56.66**	**67.65**	**65.83**	**54.95**	**63.92**	**64.54**	**67.19**	**64.95**	**65.26**	**72.11**
	GCN_10%	–	69.88	70.51	75.68	72.58	70.10	69.73	73.24	60.65	73.31	68.77	60.28	67.56	70.64	72.86	71.09	72.20	78.94
	PointRGCN_10%	–	**83.13**	**83.79**	**87.32**	**84.72**	**85.27**	**84.02**	**85.33**	**77.62**	**86.24**	**83.96**	**72.17**	**81.34**	**84.33**	**87.05**	**85.00**	**84.09**	**88.38**

time, the mean Intersect over Union (mIoU) for each sample is calculated, and the average mIoU over all instances (InsAvg) and all categories (CatAvg) are also reported.

For real-world point cloud classification experiments, overall accuracy (oAcc) and mean class accuracy (mAcc) are used as performance criteria. ‘oAcc’ represents the mean accuracy for all test instances, and ‘mAcc’ represents the mean accuracy for all shape classes [5]. Meanwhile, ‘SegAcc’, the average segmentation accuracy over all samples, is also used to evaluate the segmentation branch performance.

7.4. Pseudo labels generation results

We use the proposed PointRGCN to generate pseudo labeled data for the incompletely labeled ScanObjectN-PB_T50_RS training set. In Table 1, we report the performance of GCN and the proposed PointRGCN. Our method can correctly classify 92.2% of the total points with 10% of the labeled points. Under the setting of scarce labeling, our method can still correctly classify about 81.4% of the total points with 1% of the labeled points. Meanwhile, the PointRGCN exceeds the baseline GCN employed on the k-NN graph at different labeling levels. Moreover, by the smoothness constraint module, the misclassification can be eliminated, and only the “possibly correct” points can be retained, which further improves the accuracy.

7.5. Real-world point cloud classification results

The results of our classification framework on the ScanObjectNN-PB_T50_RS dataset are shown in Table 2. The baseline method indicates that only a few ground-truth point-level labels are used as supervision. By comparing the results of different models, we can draw the following conclusions. First of all, our method based on pseudo labels generation and noisy label learning improve the oAcc by 0.7% compared with the baseline. Secondly, our weakly supervised real-world point cloud classification network (Ours) is comparable to the fully-supervised methods [9] with only 1% point-level labels. The gap between the above two methods is only 0.3%. Finally, our method outperforms 1.5% improvement on overall accuracy compared with the DGCNN without a segmentation-guided branch.

In addition, it takes 1660 s to train our classification model for one epoch, and 0.8049 s to do inference for a batch of data, on an NVIDIA RTX3090 GPU.

7.6. Ablation analysis

We further conduct detailed experiments to evaluate the importance of proposed components, and examine the compatibility of the proposed WSC-Net with different backbone networks.

7.6.1. The importance of each component

In order to evaluate the importance of each component, we evaluate the performance of the combination of different components, and the results are summarized in Table 3. “PS” denotes that we use the generated pseudo labels as additional supervision for the segmentation branch. “SC” denotes that the smoothness constraint module is employed to refine the pseudo labels. “REG” denotes that we assign weights to $\mathcal{L}_{weak}$ and $\mathcal{L}_{pseudo}$. “NRL” denotes that we introduce the noise-robust loss to $\mathcal{L}_{pseudo}$.

Table 2
Classification results on ScanObjectNN-PB_T50_RS.

Setting	Model	oAcc	mAcc
Only shape-level labels	3DmFV [61]	63.0	58.1
	PointNet [1]	68.2	63.4
	SpiderCNN [36]	73.7	69.8
	PointNet++ [23]	77.9	75.4
	DGCNN [6]	78.1	73.6
	PointCNN [7]	78.5	75.1
Fully supervised	BGA−PN++ [9]	**80.2**	**77.5**
	BGA−DGCNN [9]	**79.9**	**75.7**
Weakly supervised	Baseline(1%)	79.0	75.0
	Ours(1%)	79.7	75.9
	Baseline(10%)	79.9	76.6
	Ours10%	**79.9**	**76.6**

Table 3
Importance of different modules.

PS	SC	REG	NRL	oAcc	mAcc	SegAcc
				79.0	75.0	78.0
x				79.0	75.3	75.9
x	x			79.4	75.8	75.7
x	x	x		79.3	**76.3**	78.0
x	x	x	x	**79.7**	75.9	**78.3**

As pseudo labels contain some misclassifications, it is difficult to train an accurate model through corrupted labels. We observe that simply summing $\mathcal{L}_{weak}$ and $\mathcal{L}_{pseudo}$ together to train the segmentation branch will not improve the classification model. Explicitly refining pseudo labels by using the smoothness constraint module leads to about 0.4% improvement for overall accuracy. By re-weighting $\mathcal{L}_{weak}$ and $\mathcal{L}_{pseudo}$, there is about 0.3% improvement compared with the baseline. Combining the above two strategies and applying noise-robust loss on pseudo label loss further improve the overall accuracy by 0.4%.

7.6.2. Compatibility

We further evaluate the compatibility with alternative backbone networks of our framework. Specifically, we conduct a compatibility experiment on PointNet++. As shown in Table 4, our method can achieve similar results under different networks. At the same time, we observe that the proposed method has a significant improvement in the segmentation accuracy compared with the baseline. However, under the 10% labeled setting, the network focuses too much on the segmentation task, and the performance on the classification task drops.

Table 4
Compatibility with alternative backbone network.

Model	SegAcc	oAcc	mAcc
PointNet++ [23]	47.37	79.17	77.02
BAG_PointNet++ [9]	–	80.20	77.50
WS_PointNet++_1%_baseline	76.01	79.48	**77.67**
WS_PointNet++_1%	**78.45**	**80.07**	77.14
WS_PointNet++_10%_baseline	77.29	**80.24**	**77.88**
WS_PointNet++_10%	**78.56**	80.14	76.97

Table 5
Classification results with different annotations.

Annotation distribution	oAcc	mAcc
Uniform_1%	79.7	75.9
Non-uniform_1%	79.5	76.0

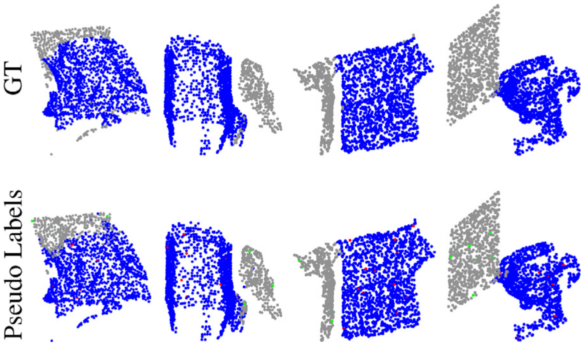

Fig. 7. 1% labeled pseudo label generation results. Zoom in to check the 1% label distribution. Foreground labels are represented by red points and background labels are represented by green points.

7.6.3. Robustness against annotation distribution

We conducted an experiment to evaluate the robustness of our framework against different annotation distributions. In the former experimental setup, we randomly choose annotation points from foreground and background parts with the same proportion, which can be seen as a uniform way. In order to evaluate robustness of our framework to non-uniform annotations, we first detect 1% keypoints as supervision for each training sample with the ISS keypoints detector [62]. Then, we use pseudo labels generated by these annotations to train the classification model. As shown in Table 5, the classification results of 1% non-uniform annotations are comparable to 1% uniform case, indicating the robustness of our weakly supervised classification framework.

7.7. Visualization

We show some qualitative results of foreground–background predictions in both pseudo labels generation on the training set and the final output segmentation results on the testing set. For each segmentation result, background and foreground points are labeled in gray and blue, respectively.

Firstly, we present the pseudo labels generation results on the scanobjectNN training set samples in Fig. 7. For each sample, the top row is the ground-truth label, and the bottom row is the pseudo labels generated with 1% point-level labels. It can be observed that our R-GCN based method can generate very accurate pseudo labels with a small amount of point-level labels. Nonetheless, we also observe that our method misclassifies some outliers.

Then, we visualize the foreground–background segmentation results of the auxiliary segmentation branch. For each sample, the top row shows the ground-truth annotations, and the bottom row shows the foreground–background predictions of our model trained with 1% ground-truth labels. Figs. 8 and 9 are the foreground–background segmentation results of correctly classified samples, and the foreground and background segmentation results of incorrectly classified samples, respectively. It can be observed that, for correctly classified samples, its segmentation results are relatively accurate. While for incorrectly classified samples, its segmentation results are relatively bad.

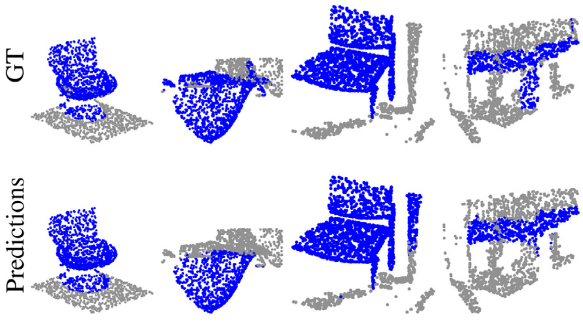

Fig. 8. Segmentation results of correctly classified samples.

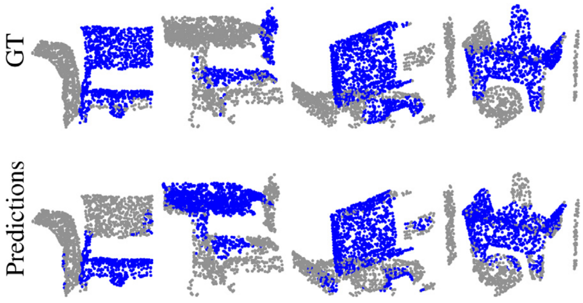

Fig. 9. Segmentation results of incorrectly classified samples.

8. Conclusion

In this paper, we propose a weakly supervised classification framework, which requires only sparse point-level foreground–background annotations, for classifying real-world point cloud objects. The proposed pseudo labels generation method Point-RGCN can significantly reduce the labor and time costs of annotating 3D real-world datasets. Besides, the introduced noise-robust multi-task loss can improve the robustness against noisy foreground–background labels. Experiments on the ScanobjectNN dataset show that our framework is comparable with many popular or state-of-the-art fully-supervised methods with only 1% point-level labels.

CRediT authorship contribution statement

An Deng: Conceptualization, Methodology, Software, Validation, Writing – original draft. **Yunchao Wu:** Software, Visualization, Writing – review & editing. **Peng Zhang:** Software, Writing – review & editing. **Zhuheng Lu:** Software, Supervision. **Weiqing Li:** Supervision. **Zhiyong Su:** Supervision, Writing – review & editing.

Declaration of competing interest

The authors declare that they have no known competing financial interests or personal relationships that could have appeared to influence the work reported in this paper.

Acknowledgments

This work was supported in part by the National Key Research and Development Program of China under Grant 2018YFB1004904, in part by the Fundamental Research Funds for the Central Universities, China under Grant 30918012203, and in part by the Science and Technology on Information System Engineering Laboratory, China under Grant 05202005. The authors would like to acknowledge the helpful comments and kindly suggestions provided by anonymous referees. Many thanks to Mikaela Angelina Uy provided ScanObjectNN real-world point cloud dataset.

References

[1] Qi CR, Su H, Mo K, Guibas LJ. Pointnet: Deep learning on point sets for 3d classification and segmentation. In: IEEE conference on computer vision and pattern recognition; 2017. p. 652–60.

[2] Xu M, Zhou Z, Qiao Y. Geometry sharing network for 3D point cloud classification and segmentation. In: Proceedings of the thirty-three AAAI conference on artificial intelligence; 2020. p. 12500–07.

[3] Ku T, Galanakis S, Boom B, Veltkamp RC, Bangera D, Gangisetty S, et al. SHREC 2021: 3D point cloud change detection for street scenes. Comput Graph 2021;99:192–200.

[4] Wang W, Su T, Liu H, Li X, Jia Z, Zhou L, et al. Surface reconstruction from unoriented point clouds by a new triangle selection strategy. Comput Graph 2019;84:144–59.

[5] Guo Y, Wang H, Hu Q, Liu H, Liu L, Bennamoun M. Deep learning for 3D point clouds: A survey. IEEE Trans Pattern Anal Mach Intell 2021;43:4338–64.

[6] Wang Y, Sun Y, Liu Z, Sarma SE, Bronstein MM, Solomon JM. Dynamic graph cnn for learning on point clouds. ACM Trans Graph 2019;38:1–12.

[7] Li Y, Bu R, Sun M, Wu W, Di X, Chen B. Pointcnn: Convolution on x-transformed points. In: Advances in neural information processing systems. 2018, p. 820–30.

[8] Xiang T, Zhang C, Song Y, Yu J, Cai W. Walk in the cloud: Learning curves for point clouds shape analysis. 2021, ArXiv Preprint arXiv:2105.01288.

[9] Uy MA, Pham Q-H, Hua B-S, Nguyen T, Yeung S-K. Revisiting point cloud classification: A new benchmark dataset and classification model on real-world data. In: International conference on computer vision; 2019. p. 1588–97.

[10] Alliegro A, Boscaini D, Tommasi T. Joint supervised and self-supervised learning for 3D real-world challenges. 2020, ArXiv Preprint arXiv:2004.07392.

[11] Fuchs F, Worrall D, Fischer V, Welling M. SE (3)-transformers: 3D roto-translation equivariant attention networks. In: Advances in neural information processing systems. 33, 2020, p. 1970–81.

[12] Zhao C, Yang J, Xiong X, Zhu A, Cao Z, Li X. Rotation invariant point cloud classification: Where local geometry meets global topology. 2019, ArXiv Preprint, arXiv:1911.00195.

[13] Mo K, Zhu S, Chang AX, Yi L, Tripathi S, Guibas LJ, et al. Partnet: A large-scale benchmark for fine-grained and hierarchical part-level 3d object understanding. In: IEEE conference on computer vision and pattern recognition; 2019. p. 909–18.

[14] Armeni I, Sener O, Zamir AR, Jiang H, Brilakis I, Fischer M, et al. 3d semantic parsing of large-scale indoor spaces. In: IEEE conference on computer vision and pattern recognition; 2016. p. 1534–43.

[15] Hackel T, Savinov N, Ladicky L, Wegner JD, Schindler K, Pollefeys M. Semantic3d. net: A new large-scale point cloud classification benchmark. 2017, ArXiv Preprint arXiv:1704.03847.

[16] Zhou Z-H. A brief introduction to weakly supervised learning. Natl Sci Rev 2018;5:44–53.

[17] Su H, Maji S, Kalogerakis E, Learned-Miller E. Multi-view convolutional neural networks for 3d shape recognition. In: IEEE international conference on computer vision; 2015. p. 945–53.

[18] Feng Y, Zhang Z, Zhao X, Ji R, Gao Y. Gvcnn: Group-view convolutional neural networks for 3d shape recognition. In: IEEE conference on computer vision and pattern recognition; 2018. p. 264–72.

[19] Ma C, Guo Y, Yang J, An W. Learning multi-view representation with LSTM for 3-D shape recognition and retrieval. IEEE Trans Multimed 2018;21:1169–82.

[20] Goyal A, Law H, Liu B, Newell A, Deng J. Revisiting point cloud shape classification with a simple and effective baseline. 2021, ArXiv Preprint arXiv:2106.05304.

[21] Wu Z, Song S, Khosla A, Yu F, Zhang L, Tang X, Xiao J. 3d shapenets: A deep representation for volumetric shapes. In: IEEE conference on computer vision and pattern recognition; 2015. p. 1912–20.

[22] Maturana D, Scherer S. Voxnet: A 3d convolutional neural network for real-time object recognition. In: IEEE international conference on intelligent robots and systems; 2015. p. 922–28.

[23] Qi CR, Yi L, Su H, Guibas LJ. Pointnet++: Deep hierarchical feature learning on point sets in a metric space. In: Advances in neural information processing systems. 2017, p. 5099–108.

[24] Li J, Chen BM, Hee Lee G. So-net: Self-organizing network for point cloud analysis. In: IEEE conference on computer vision and pattern recognition; 2018. p. 9397–406.

[25] Munoz D, Vandapel N, Hebert M. Directional associative markov network for 3-d point cloud classification. In: International symposium on 3D data processing, visualization and transmission; 2008. p. 63–70.

[26] Niemeyer J, Rottensteiner F, Soergel U. Conditional random fields for lidar point cloud classification in complex urban areas. ISPRS Ann Photogramm Remote Sens Spat Inf Sci 2012;1:263–8.

[27] Simonovsky M, Komodakis N. Dynamic edge-conditioned filters in convolutional neural networks on graphs. In: IEEE conference on computer vision and pattern recognition; 2017. p. 3693–702.

[28] Zhang Y, Rabbat M. A graph-cnn for 3d point cloud classification. In: IEEE international conference on acoustics, speech and signal processing; 2018. p. 6279–83.

[29] Wang C, Samari B, Siddiqi K. Local spectral graph convolution for point set feature learning. In: Proceedings of the European conference on computer vision; 2018. p. 52–66.

[30] Landrieu L, Simonovsky M. Large-scale point cloud semantic segmentation with superpoint graphs. In: IEEE conference on computer vision and pattern recognition; 2018. p. 4558–67.

[31] Te G, Hu W, Zheng A, Guo Z. Rgcnn: Regularized graph cnn for point cloud segmentation. In: Proceedings of the 26th ACM international conference on multimedia; 2018. p. 746–54.

[32] Li G, Muller M, Thabet A, Ghanem B. Deepgcns: Can gcns go as deep as cnns?. In: IEEE international conference on computer vision; 2019. p. 9267–76.

[33] Thomas H, Qi CR, Deschaud J-E, Marcotegui B, Goulette F, Guibas LJ. Kpconv: Flexible and deformable convolution for point clouds. In: IEEE international conference on computer vision; 2019. p. 6411–20.

[34] Wu W, Qi Z, Fuxin L. Pointconv: Deep convolutional networks on 3d point clouds. In: IEEE conference on computer vision and pattern recognition; 2019. p. 9621–30.

[35] Mao J, Wang X, Li H. Interpolated convolutional networks for 3d point cloud understanding. In: IEEE international conference on computer vision; 2019. p. 1578–87.

[36] Xu Y, Fan T, Xu M, Zeng L, Qiao Y. Spidercnn: Deep learning on point sets with parameterized convolutional filters. In: Proceedings of the European conference on computer vision; 2018. p. 87–102.

[37] Hua B-S, Tran M-K, Yeung S-K. Pointwise convolutional neural networks. In: IEEE Conference on computer vision and pattern recognition; 2018. p. 984–93.

[38] Xu M, Ding R, Zhao H, Qi X. PAConv: Position adaptive convolution with dynamic kernel assembling on point clouds. In: IEEE conference on computer vision and pattern recognition; 2021. p. 3173–82.

[39] Liu K, Gao Z, Lin F, Chen BM. Fg-net: Fast large-scale LiDAR point CloudsUnderstanding network leveraging CorrelatedFeature mining and geometric-aware modelling. 2020, ArXiv Preprint arXiv:2012.09439.

[40] Qiu S, Anwar S, Barnes N. Dense-resolution network for point cloud classification and segmentation. In: IEEE winter conference on applications of computer vision; 2021. p. 3813–22.

[41] Li X, Yu L, Fu C-W, Cohen-Or D, Heng P-A. Unsupervised detection of distinctive regions on 3D shapes. ACM Trans Graph 2020;39:1–14.

[42] Thabet A, Alwassel H, Ghanem B. Self-supervised learning of local features in 3d point clouds. In: IEEE conference on computer vision and pattern recognition workshops; 2020. p. 938–9.

[43] Sauder J, Sievers B. Self-supervised deep learning on point clouds by reconstructing space. In: Advances in neural information processing systems. 2019, p. 12962–72.

[44] Xu X, Lee GH. Weakly supervised semantic point cloud segmentation: Towards 10x Fewer Labels. In: IEEE conference on computer vision and pattern recognition; 2020. p. 13706–15.

[45] Wei J, Lin G, Yap K-H, Hung T-Y, Xie L. Multi-Path Region Mining For Weakly Supervised 3D Semantic Segmentation on Point Clouds, In: IEEE conference on computer vision and pattern recognition; 2020. p. 4384–93.

[46] Vahdat A. Toward robustness against label noise in training deep discriminative neural networks. In: Advances in neural information processing systems. 2017, p. 5596–605.

[47] Lee K-H, He X, Zhang L, Yang L. Cleannet: Transfer learning for scalable image classifier training with label noise. In: IEEE conference on computer vision and pattern recognition; 2018. p. 5447–56.

[48] Li Y, Yang J, Song Y, Cao L, Luo J, Li L-J. Learning from noisy labels with distillation. In: IEEE conference on computer vision and pattern recognition; 2017. p. 1910–18.

[49] Jiang L, Zhou Z, Leung T, Li L-J, Fei-Fei L. Mentornet: Learning data-driven curriculum for very deep neural networks on corrupted labels. In: International conference on machine learning; 2018. p. 2304–13.

[50] Han B, Yao Q, Yu X, Niu G, Xu M, Hu W, et al. Co-teaching: Robust training of deep neural networks with extremely noisy labels. In: Advances in neural information processing systems. 2018, p. 8527–37.

[51] Tanaka D, Ikami D, Yamasaki T, Aizawa K. Joint optimization framework for learning with noisy labels. In: IEEE conference on computer vision and pattern recognition; 2018. p. 5552–60.

[52] Han B, Yao J, Niu G, Zhou M, Tsang I, Zhang Y, et al. Masking: A new perspective of noisy supervision. In: Advances in neural information processing systems. 2018, p. 5836–46.

[53] Ma X, Huang H, Wang Y, Romano S, Erfani S, Bailey J. Normalized loss functions for deep learning with noisy labels. In: International conference on machine learning; 2020. p. 6543–53.

[54] Ghosh A, Kumar H, Sastry P. Robust loss functions under label noise for deep neural networks. In: The thirty-first AAAI conference on artificial intelligence; 2017. p. 1919–25.

[55] Zhang Z, Sabuncu M. Generalized cross entropy loss for training deep neural networks with noisy labels. In: Advances in neural information processing systems. 2018, p. 8778–88.

[56] Wang Y, Ma X, Chen Z, Luo Y, Yi J, Bailey J. Symmetric cross entropy for robust learning with noisy labels. In: IEEE conference on computer vision and pattern recognition; 2019. p. 322–30.

[57] Huang R, Hong D, Xu Y, Yao W, Stilla U. Multi-scale local context embedding for LiDAR point cloud classification. IEEE Geosci Remote Sens Lett 2019;17:721–5.

[58] Schlichtkrull MS, Kipf T, Bloem P, Den Berg RV, Titov I, Welling M. Modeling relational data with graph convolutional networks. In: European semantic web conference; 2018. p. 593–607.

[59] Lee D-H. Pseudo-label: The simple and efficient semi-supervised learning method for deep neural networks. In: Workshop on challenges in representation learning, ICML, vol. 3; 2013. p. 2.

[60] Dai A, Chang AX, Savva M, Halber M, Funkhouser T, Nießner M. Scannet: Richly-annotated 3d reconstructions of indoor scenes. In: IEEE conference on computer vision and pattern recognition; 2017. p. 5828–39.

[61] Ben-Shabat Y, Lindenbaum M, Fischer A. 3Dmfv: Three-dimensional point cloud classification in real-time using convolutional neural networks. IEEE Robot Autom Lett 2018;3(4):3145–52.

[62] Zhong Y. Intrinsic shape signatures: A shape descriptor for 3d object recognition. In: 2009 IEEE 12th international conference on computer vision workshops, ICCV workshops; 2009. p. 689–96.

An Deng

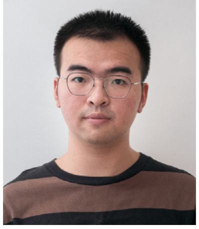

Peng Zhang

Zhuheng Lu

Weiqing Li

Zhiyong Su